12

Probabilistic Method to Estimate Design Accelerograms in Seville and Granada Based on Uniform Seismic Hazard Response Spectra

José Luis de Justo[1*], Antonio Morales-Esteban[1*],
Francisco Martínez-Álvarez[2] and J. M. Azañón[3]
[1]*Department of Continuum Mechanics, University of Seville*
[2]*Department of Computer Science, Pablo de Olavide University of Seville*
[3]*Department of Geodynamics, University of Granada*
Spain

1. Introduction

The response of a structure affected by an earthquake is the result of "filtering" the seismic signal through the structure. A dynamic analysis of a structure requires the previous definition of the accelerogram and the structure characteristics. A complete calculation implies working out the seismic response in all points of the structure; that is, calculating the seismic response in an infinite number of points and in an infinite number of instants. (Meirovitch, 1985) has demonstrated that, with an infinite number of points and instants, the problem has no numerical solution. To solve the numerical problem, models with a finite number of predeterminated points are defined.

The response of a structure subject to a seismic movement can be determined by two methods: either using the accelerograms recorded near the site, or using visco-elastic response spectra.

The first method can only be used in places where many accelerograms have been recorded, and needs a probabilistic calculation to ascertain the design accelerograms. This procedure can be used for linear and non-linear analyses. In both cases various records of a frequency similar to that expected at the location of the structure, may be used to obtain realistic calculation results. A structural analysis for all the accelerograms considered must be carried out in order to obtain a calculation envelope or carry out the probabilistic study. This procedure implies a significant work. This procedure has the difficulty of finding accelerograms at the location of the structure. In some regions, with a vast history of large earthquakes, such as Japan and California, a wide network of recording stations is available and provides many records for large earthquakes, for different type of soils and for a wide range of distances. In regions of minor seismicity, the network of recording stations is not so wide, or is not old enough, so that the number of records is insufficient. For the analysis of minor seismic activity regions, records from other regions are used, or artificial accelerograms are generated. Artificial accelerograms have the advantage that, from a minimum number of parameters, accelerograms can be obtained.

[*] Both Authors contributed equally

Once between 5 and 10, real or artificial, accelerograms have been obtained, they must be scaled to a level of severity. The most commonly used method consists of scaling the seismic peak acceleration up to a predetermined probabilistic level. However, the potential damage an earthquake can produce is not only a function of the peak acceleration so this method is not suitable for a linear calculation. There are many alternatives such as the Arias intensity and the spectral intensity of Housner, (Housner, 1975; Lin & Mahin, 1985) more related to the potential damage.
The use of visco-elastic response spectra is more adequate to obtain accelerograms in regions where the number of records is insufficient, as the response spectrum is the soil movement parameter better related to the structural response. This is the most commonly used method due to its simplicity and appropriate accuracy, as the response of structures, in the elastic linear range, can be obtained as the superposition of a few modes of vibration.
A probabilistic method for estimating the calculation accelerograms is presented in this paper. First, uniform seismic hazard response spectra in Seville and Granada are obtained. Based on them, the calculation accelerograms can be obtained.

2. Fundamentals

Seismic hazard can be defined as the probability of exceeding a parameter of the soil movement, produced by an earthquake, in a location and in a period of time. To unify criteria, UNESCO proposed the commonly accepted definition, given by (UNDRO, 1979). Hazard (H) is defined by a probability function of the characteristic parameter of the soil movement (S) at a location (x) according to:

$$H = P\left[S(x) \geq S_o; t\right] \tag{1}$$

P represents the probability of exceeding a threshold value (S_0) of the characteristic parameter of the soil movement during the time (t).
There are two methods for evaluating the seismic hazard: the deterministic method and the probabilistic method.

2.1 Deterministic method

The deterministic method assumes the hypothesis that the seismicity is stationary, considering that earthquakes in the future will be similar to those in the past and estimate the upper limit of the movement, expressed as the maximum value of the parameter. These earthquakes can be real earthquakes that in the past affected the location, or can be deduced from the seismic and tectonic characteristics of the area. The deterministic method can be divided into zoned or not-zoned, in function of how the seismicity distribution is considered. This method presents some advantages and disadvantages. Its main advantage is its easy application. It defines earthquakes that happened in the past and it is easy to suppose that similar earthquakes will happen in the future. However, the probability that those earthquakes will happen is, generally, unknown. The deterministic method estimates the largest earthquake that can affect the location, while the rest of earthquakes are not considered. The sources are characterized by the largest earthquake, and not by its recurrence law.
The calculation procedure is (Benito & Jiménez, 1999):

1. Definition of the influence area of the location, and identification of the seismic sources or faults within it.
2. Estimation of the largest earthquakes happened in the influence area, or at any of the source areas.
3. Estimation of the seismic parameter at the location, caused by the maximum potential earthquakes of every area or of the whole area.
4. Determination of the hazard at the location, taking the maximum value generated by the influence areas. Hazard is defined by the upper limit of the movement at the location.

2.2 Probabilistic method

The probabilistic methods sum up the contribution of all the possible earthquakes that can affect a location, and consider recurrence laws for them. As a result, the probability of exceeding every value of a parameter of the soil movement expected at the location, during a period of time, is estimated. The hazard is represented by probability curves. These methods are classified into parametric and non-parametric, according to the statistical distribution adopted.

2.2.1 Non-parametric methods

These methods analyze the hazard according to extreme value distribution functions. The most used were defined by (Gumbel, 1958). The method is based on the following steps:

1. Definition of the area of influence around the location.
2. Calculation of the values of the seismic parameter at the location, applying attenuation laws to the values of the parameter, that reflect the seismicity of the area during the period of time considered.
3. Adjustment to a distribution of extreme values of the random parameter, defined with the values of the estimated parameter, and estimation of the distribution coefficients.
4. Estimation of the probability of exceeding the extreme value, during the time considered, calculating, this way, the probability.

2.2.2 Parametric methods

The methodology was initially proposed by Cornell (1968). The method is based on the existence of different seismogenic areas. First, the influence area is divided into seismogenic areas and the seismicity of every area is adjusted according to a recurrence law. Later, the contribution of all the sources is summed up to obtain a probability function that represents the hazard at the location.

3. Methodology

3.1 Probabilistic method to estimate seismic hazard

Seismic hazard is presented by means of a hazard function (H) that indicates the characteristic parameter of the soil movement (S), according to the following formula:

$$H(S_0;t) = P(S \geq S_0;t) \tag{2}$$

Where $P(S \geq S_0;t)$ is the probability that the characteristic parameter of the soil movement will exceed a threshold value, S_0, at least once during the time, t.

The arrival of earthquakes to a location is assumed to follow a Poisson´s stationary process (Cornell, 1968; Veneziano et al., 1984). Under this hypothesis, the hazard function can be expressed as follows:

$$H(S_0;t) = 1 - e^{-\lambda(S_0)t} \tag{3}$$

where $\lambda(S_0)$ is the annual rate of times that the parameter (S_0) has been exceeded at the location.

To carry out a study of the seismic hazard, a database of earthquakes that can affect the location must be provided. If the value of the characteristic parameter of the soil movement, during every one of these earthquakes is known and the database is complete, even with the largest earthquakes that can affect the location, the annual rate of exceeding could be calculated according to the following formula:

$$\lambda(S_0) = \frac{1}{t_c}\sum_k \delta(S_k - S_0) \tag{4}$$

Where t_c is the duration of the database, S_k is the value of the characteristic parameter of the soil movement during the k earthquake of the database, and δ is Heaviside´s function:

$$\delta(S_k - S_0) = \begin{cases} 1 \rightarrow S_k - S_0 \geq 0 \\ 0 \rightarrow S_k - S_0 < 0 \end{cases} \tag{5}$$

The formula (4) provides a good estimation of $\lambda(S_0)$ only if all the earthquakes, that can affect the location, have been presented various times during the period of time the database covers. This implies that the database should have a very long duration, probably of thousands of years (Ebel & Kafka, 1999).

If an instrumental parameter is taken as characteristic of the soil movement, the annual rate of exceeding $\lambda(S_0)$ can't be obtained by means of (4) as there are no databases of enough duration.

In this case, the seismic sources and the attenuation laws of the soil movement, from the source to the location, must be analyzed. The steps to follow with this methodology were proposed by (Cornell, 1968):

1. Seismicity model: definition of the seismogenic areas that can affect the site. If the seismicity can be considered homogenous in the whole seismogenic area, a unique seismicity source of global influence can be defined.
2. Recurrence model. The recurrence model in every seismogenic area must be defined. If it is admitted that the seismicity is distributed randomly and it adjusts to the Gutenberg-Richter law with upper truncation, the parameters of the law (a and b) are characteristics of the model. Moreover, for every area maximum and minimum magnitudes are defined that establishes the validity limits of the model.
3. Attenuation law. Attenuation laws to obtain the selected parameter in function of the distance must be determined in order to evaluate the seismic hazard. The application of these laws over the seismicity of every area, represented by its recurrence law, allows obtaining the result over the site.
4. Probabilistic hazard equation. The estimation of the total hazard is obtained adding up the probabilities obtained by the result of all the areas that affect the site.

$$H = \sum_{i=1}^{n} \left(1 - e^{-t\lambda}\right) \tag{6}$$

Where λ is the annual rate of earthquakes, occurring in any area, that produce a parameter of the soil movement superior to the reference one at the studied site, n is the number of areas and t is the period of time, in years, considered.
The uniform seismic hazard response spectra are those that have the same probability of being exceeded in all the periods, obtained with the methodology proposed by (Cornell, 1968).

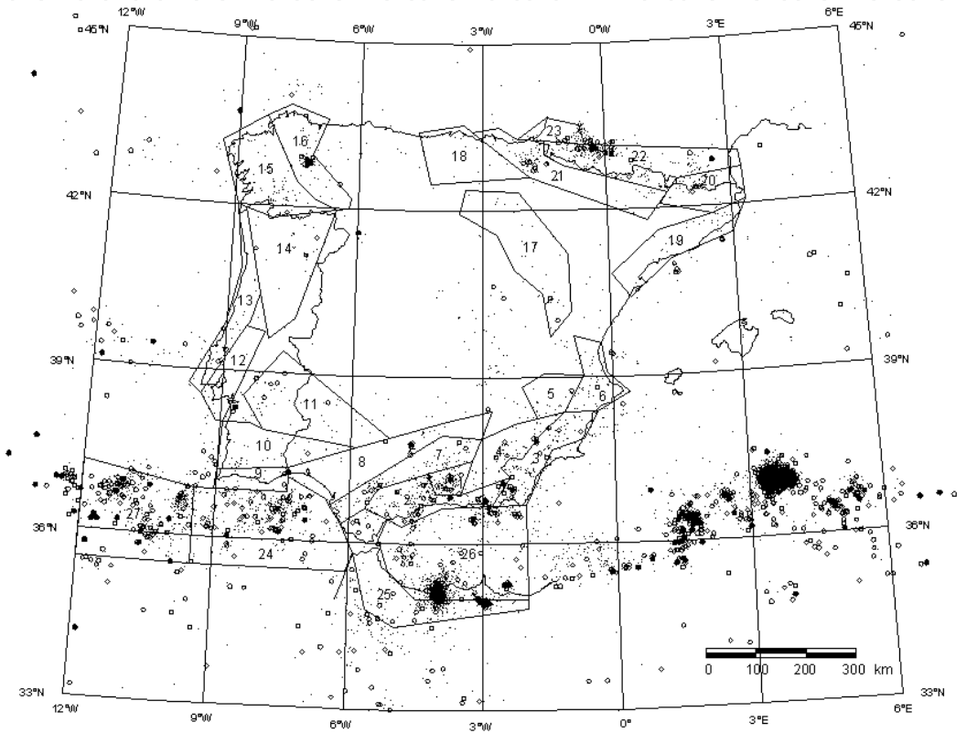

Fig. 1. Seismogenic areas of Spain and Portugal. Dots represent earthquakes of moment magnitude between 3.0 and 4.0, circles between 4.0 and 5.0, and solid circles of magnitude larger than 5.0.

3.1.1 Seismicity model

Seismicity is defined as the whole description of the seismic phenomena in its origin (Martín, 1984). Seismicity can be assimilated to a process of punctual events that result from the relaxation of stress that acts over an area. For its study, the spatial distribution of the earthquakes and its occurrence, according to time, must be known. The most appropriate way to study the irregularities of the temporal series of the earthquakes is through a statistical model.
The model used in this text is based on the seismogenic areas defined by (Martín, 1984). A seismogenic area is a source of earthquakes with homogenous seismic and tectonic characteristics. The process of earthquakes generation is spatially and temporary homogenous in every area. The twenty seven areas established for the Iberian Peninsula are based on tectonic, geological, seismic and gravimetrical data. The twenty seven areas are described in Table 1 and Figure 1.

3.1.2 Recurrence model

The seismicity in every seismogenic area is randomly distributed and it adjusts to the Gutenberg-Richter law. The Gutenberg-Richter law must be truncated, with upper and lower limits, in seismic hazard studies, to consider the magnitude, M_{max}, of the largest earthquake that can occur at the source, and to avoid considering earthquakes of magnitude less than M_{min} respectively. The probability density function of magnitude for Gutenberg-Richter law is:

$$f(M) = \beta \frac{e^{\beta(M-M_{min})}}{1-e^{\beta(M_{max}-M_{min})}} \tag{7}$$

The seismicity in every seismogenic area is defined by the following parameters:

1. The maximum and minimum magnitude.
2. The annual rate of earthquakes occurrence between M_{max} and M_{min}.
3. The *b*-value of the Gutenberg-Richter law.

Area	Description
1	Granada basin
2	Penibetic area
3	Area to the East of the Betic system
4	Quaternary Guadix-Baza basin
5	Area of moderate seismicity to the North of the Betic System
6	Area of moderate seismicity including the Valencia basin
7	Sub-betic area
8	Tertiary basin in the Guadalquivir depression
9	Algarve area
10	South-Portuguese unit
11	Ossa Morena tectonic unit
12	Lower Tagus Basin
13	West Portuguese fringe
14	North Portugal
15	West Galicia
16	East Galicia
17	Iberian mountain mass
18	West of the Pyrenees
19	Mountain range of the coast of Catalonia
20	Eastern Pyrenees
21	Southern Pyrenees
22	North Pyrenees
23	North–Eastern Pyrenees
24	Eastern part of Azores–Gibraltar fault
25	North Morocco and Gibraltar field
26	Alboran Sea
27	Western Azores–Gibraltar fault

Table 1. Seismogenic areas of Spain and Portugal

The maximum magnitude in every seismogenic area has been determined by (Martín, 1984) from seismic and tectonic considerations. The minimum magnitude in all areas is 5.0. Lower earthquakes are not considered dangerous. The *b*-value and the annual rate of earthquakes can be obtained from Table 2.

Area	*b*-value	Annual rate of earthquakes	Surface (km²)	Anual rate / surface (km²)
1	1.41	5.14	3835	1.34E-03
2	1.18	7.82	13979	5.59E-04
3	1.29	4.36	13251	3.29E-04
4	1.27	2.26	11957	1.89E-04
5	1.62	0.87	7066	1.24E-04
6	2.17	1.38	9735	1.42E-04
7	1.51	4.32	13954	3.10E-04
8	0.92	1.47	22228	6.63E-05
9	1.20	0.77	6371	1.21E-04
10	2.33	2.56	15717	1.63E-04
11	1.44	2.35	27694	8.47E-05
12	1.01	0.50	9803	5.08E-05
13	1.29	1.41	13029	1.09E-04
14	1.40	1.75	26049	6.71E-05
15	2.07	4.02	22597	1.78E-04
16	1.54	2.87	15475	1.85E-04
17	1.75	1.07	26993	3.96E-05
18	1.54	0.58	15738	3.70E-05
19	1.90	1.18	16032	7.35E-05
20	1.63	1.68	10622	1.58E-04
21	1.53	2.63	19946	1.32E-04
22	1.48	12.32	22383	5.51E-04
23	1.46	2.06	4301	4.78E-04
24	0.96	13.55	46329	2.92E-04
25	0.96	5.85	24600	2.38E-04
26	1.14	18.21	48669	3.74E-04
27	0.70	15.16	38955	3.89E-04

Table 2. Annual rate of earthquakes and *b*-value for the seismogenic areas of Spain and Portugal

3.1.3 Attenuation model

The characteristic parameter of the soil movement is the acceleration or relative velocity response spectrum for 0, 2, 5, 10 or 20 percent damping. The coefficients for the attenuation laws can be obtained from (Morales-Esteban, 2010).

3.1.4 Probabilistic hazard equation

It is admitted that the arrival at the site of earthquakes that exceed the reference value, log S_0, follows a Poisson stationary process, defined by Gutenberg-Richter law of constant λ_i:

$$\lambda_i = \upsilon_i \int_{M_{\min}}^{M_{\max}} P\left(\log S \geq \log S_0 / M, D\right) f\left(M\right) dM \tag{8}$$

The seismic rate of the punctual source is υ_i and *f(M)* is the probability density function of magnitude (equation 7).

If N punctual seismic sources hit simultaneously the site, the rate λ of arrivals at the location that exceed the reference value log S_0 is:

$$\lambda = \sum_{i=1}^{N} \lambda_i \tag{9}$$

The probability of exceeding the reference value $logS_0$ during a time t caused by the simultaneous action of N punctual seismic sources is:

$$P\left(\log S \geq \log S_0 ; t\right) = 1 - e^{-\lambda t} \tag{10}$$

Its return period can be obtained from:

$$T = \frac{1}{\lambda} = \frac{-t}{\ln\left(1 - P\left(\log S \geq \log S_0 ; t\right)\right)} \tag{11}$$

Equation (10) can't be applied to the hazard calculation as the seismogenic areas have been modeled as areas and not as punctual seismic sources. To solve this problem, the seismogenic areas are divided into elements small enough to be assimilated to punctual seismic sources (Figure 2).

Every seismogenic area is divided into N square elements, small enough, so that the seismicity of every one of these squares is assumed to be concentrated in its center. Every seismogenic area is divided into N punctual seismic sources. Every one of them has an earthquake occurrence rate $\upsilon_i = \upsilon / N$, where υ is the seismic rate of the whole seismogenic area.

3.2 Resolution of the hazard probabilistic equation

A computer program that divides the seismogenic areas into punctual seismic sources that affect a site, that integrates numerically equation (8) and calculates the probability of exceeding with equation (10) has been developed.

With this method the probability of exceeding has been calculated for some values of the acceleration response spectra for an exposure time of 50 and 100 years for the cities of Seville as Granada. This way a hazard plot of seismic hazard is obtained and is shown in Figure 3. If this process is repeated for various periods of the structure and, for every hazard plot, the spectrum curve for the same probability of exceeding is obtained, and a uniform seismic hazard response spectrum can be obtained, point by point, as shown in Figure 4.

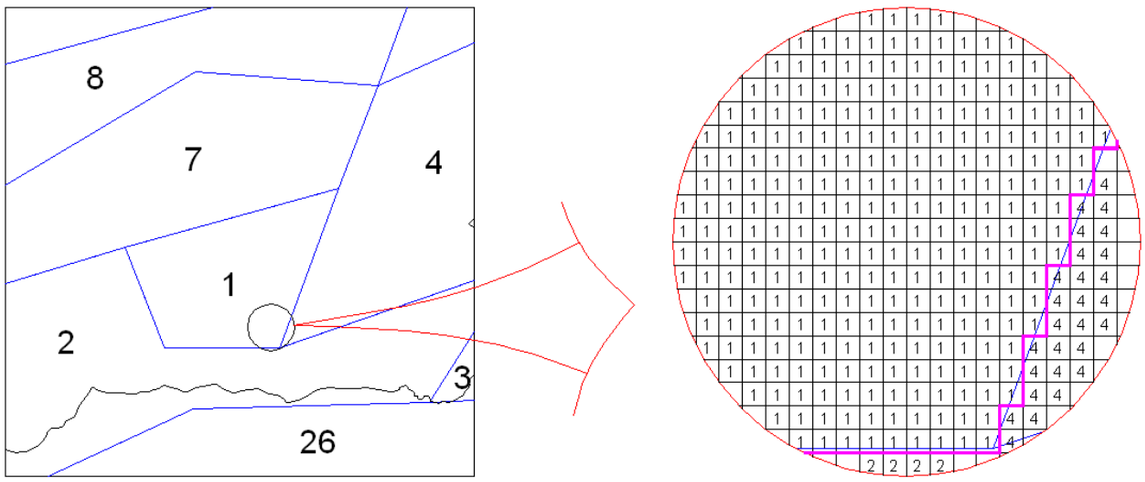

Fig. 2. Scheme of division of a seismogenic area into N punctual areas, through an orthogonal mesh.

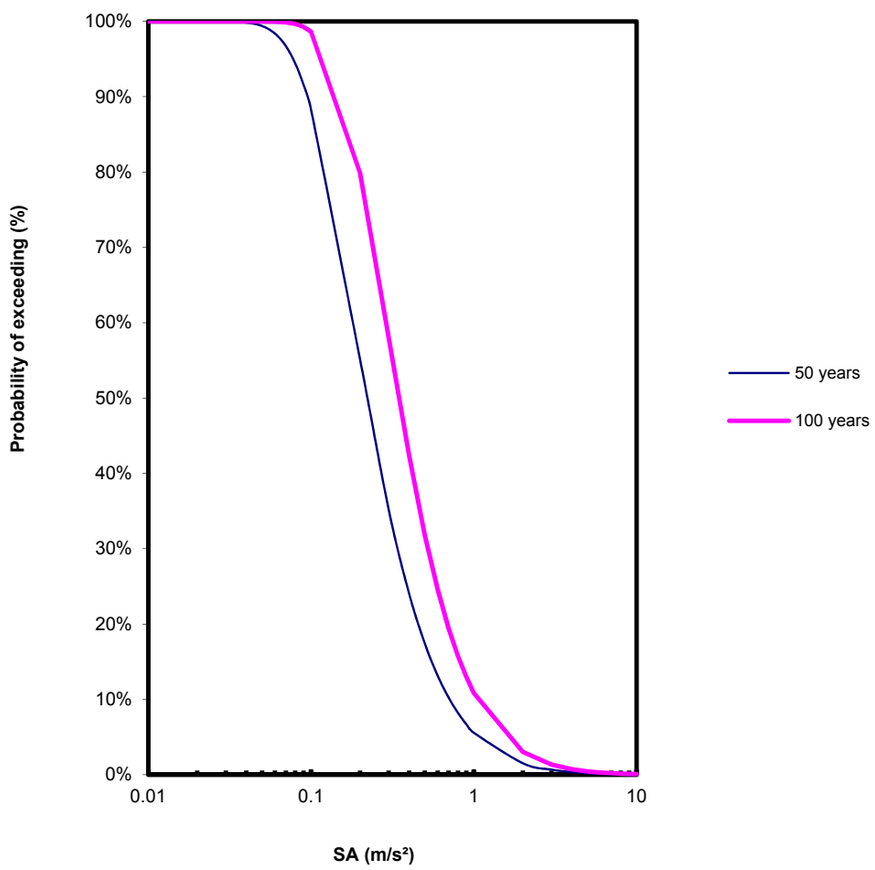

Fig. 3. Seismic hazard plot for Seville site; exposure times 50 and 100 years, respectively; natural period of structure 0.50 s; type of soil rock and relative damping 5%.

3.3 Application to Seville and Granada

Seismic hazard curves for the acceleration spectra in Seville and Granada have been obtained. Figures 5 and 6 show the curves for a period of 0.5 s, for a 5% relative damping and a time of exposure of 50 years, as a function of the soil type for Granada and Seville, respectively. Figure 7 compares the seismic hazard curves for Granada, as a function of the relative damping, for an acceleration response spectrum of period 0.20 s and for a time of exposure of 50 years. Figure 8 represents the hazard curves for Seville and Granada in hard soil for a period of 0.50 s, a relative damping of 5% and an exposure time of 50 years. Figure 9 compares the seismic hazard curves for Granada as a function of the time of exposure (50 and 100 years) in rock, for a period of 0.50 s and a relative damping of 5%.

Following the methodology described in this text, the uniform seismic hazard acceleration response spectra for the cities of Seville and Granada, for a relative damping of the 5%, a probability of exceeding of the 5% and a time of exposure of 50 years, which is equivalent to a return period of 975 years, have been obtained. In figures 10 and 11, the uniform seismic hazard response spectra for Granada and Seville, respectively, are compared as a function of the soil type. Figures 12, 13 and 14 compare the uniform seismic hazard response spectra in rock, hard soil and soft soil, respectively, for the two sites (Seville and Granada).

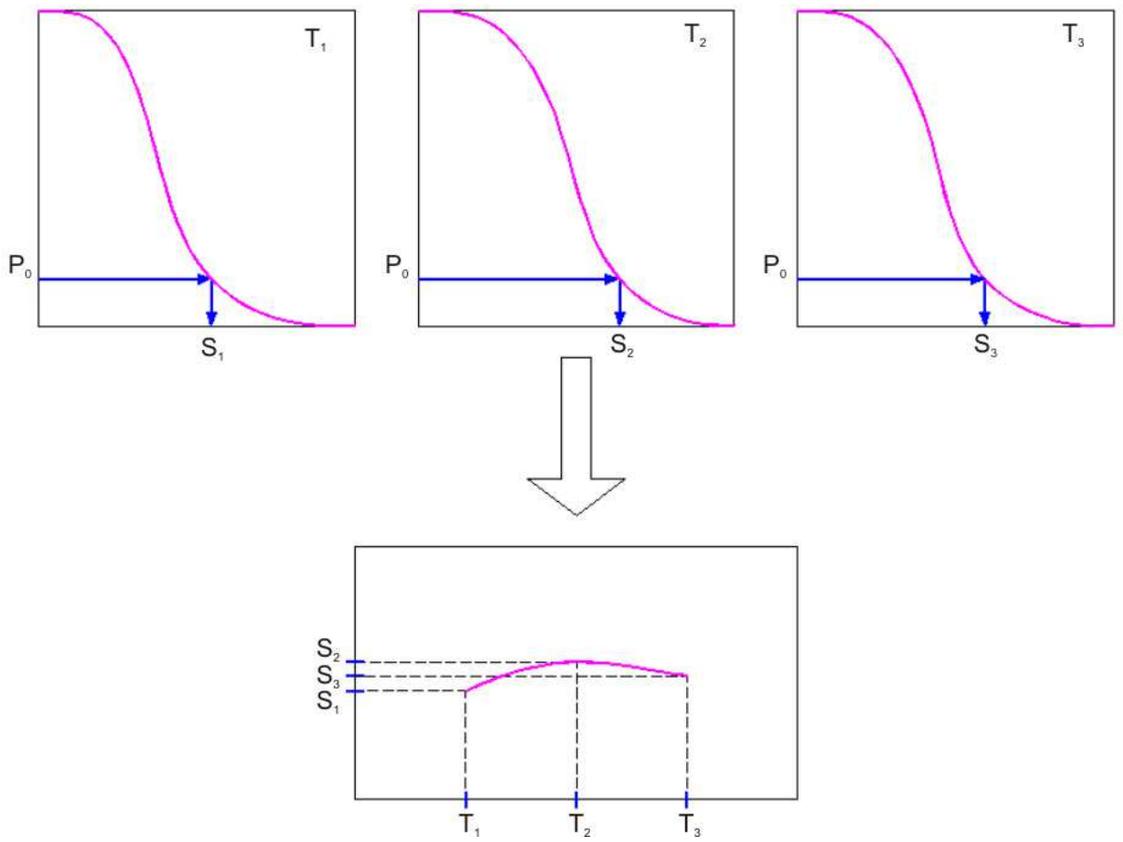

Fig. 4. Scheme of construction of a uniform seismic hazard response spectrum from the seismic hazard plots.

3.4 Assessment of design accelerograms

The procedure to estimate design accelerograms is:

1. The time of exposure of structure is established according to the hazard level.
2. The admitted probability of exceeding is established, normally a 5-10%, according to the hazard level.
3. The uniform seismic hazard acceleration response spectra for the site are calculated according to the type of soil and the required level of hazard (time of exposure and probability of exceeding).
4. In the database of accelerograms, registered in the same type of soil of the site, records are examined. The scale factor, f, between the logarithm of the calculated uniform seismic hazard spectrum and the logarithm of the response spectrum corresponding to the real spectrum, that minimizes the standard deviation, s, is calculated.

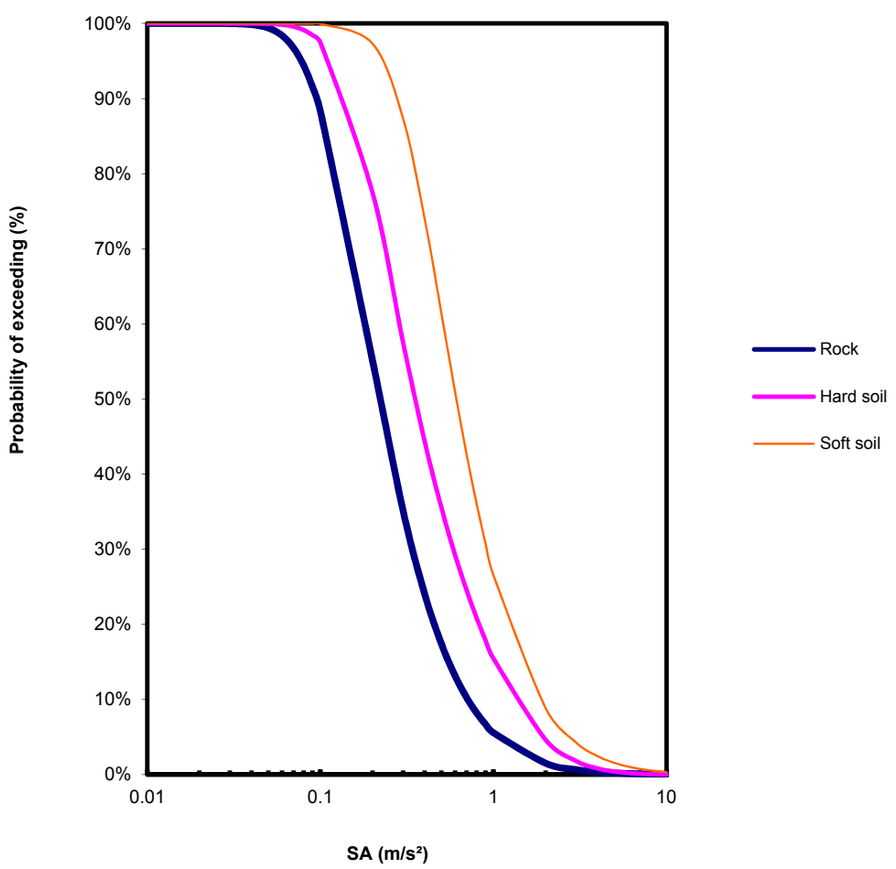

Fig. 5. Comparison of the seismic hazard plot of the acceleration response spectra of period 0.50 s for Granada for different soil types, for a 5% relative damping and a time of exposure of 50 years.

So, if S_R is the response spectrum correspondent to the real register, and S_C is the calculated response spectrum, the standard deviation is:

$$s = \sqrt{\frac{\sum\left[\log\left(f \cdot S_R\right) - \log\left(S_C\right)\right]^2}{25}} \tag{12}$$

The scale factor that minimizes the standard deviation is:

$$f = \frac{\Sigma \log S_C - \Sigma \log S_R}{25} \tag{13}$$

The sum is extended to the 25 periods for which the uniform seismic hazard response spectrum has been calculated.

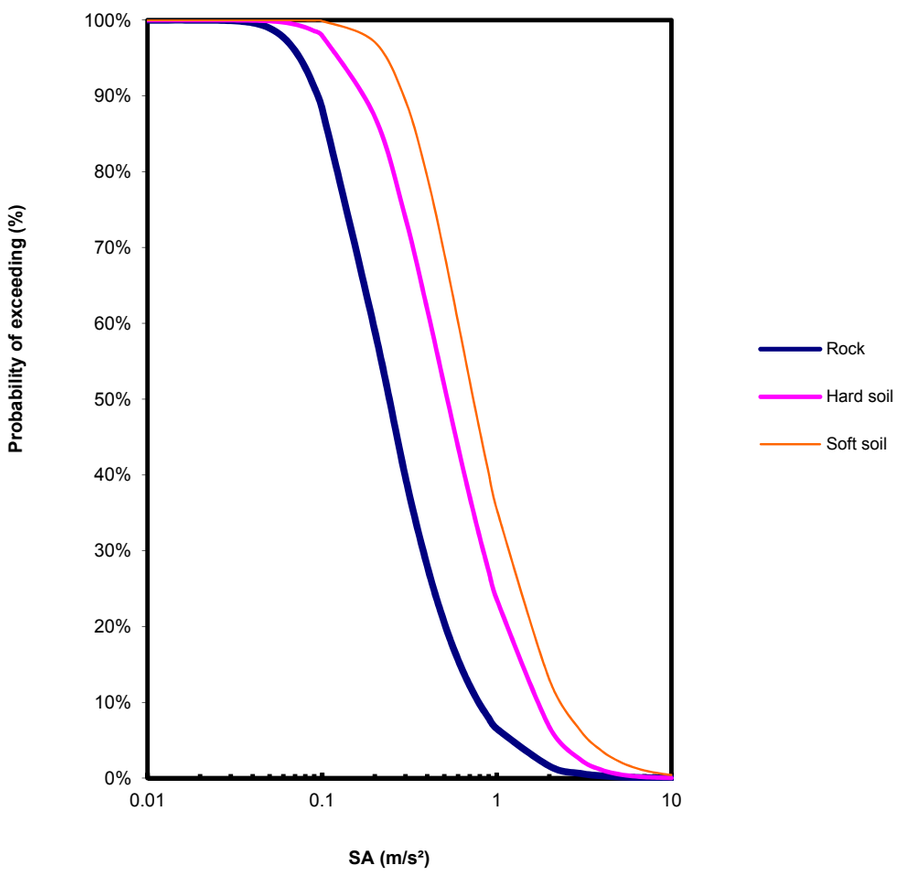

Fig. 6. Comparison of the seismic hazard plot of the acceleration response spectra of period 0.50 s for Seville for different soil types, for a 5% relative damping and a time of exposure of 50 years.

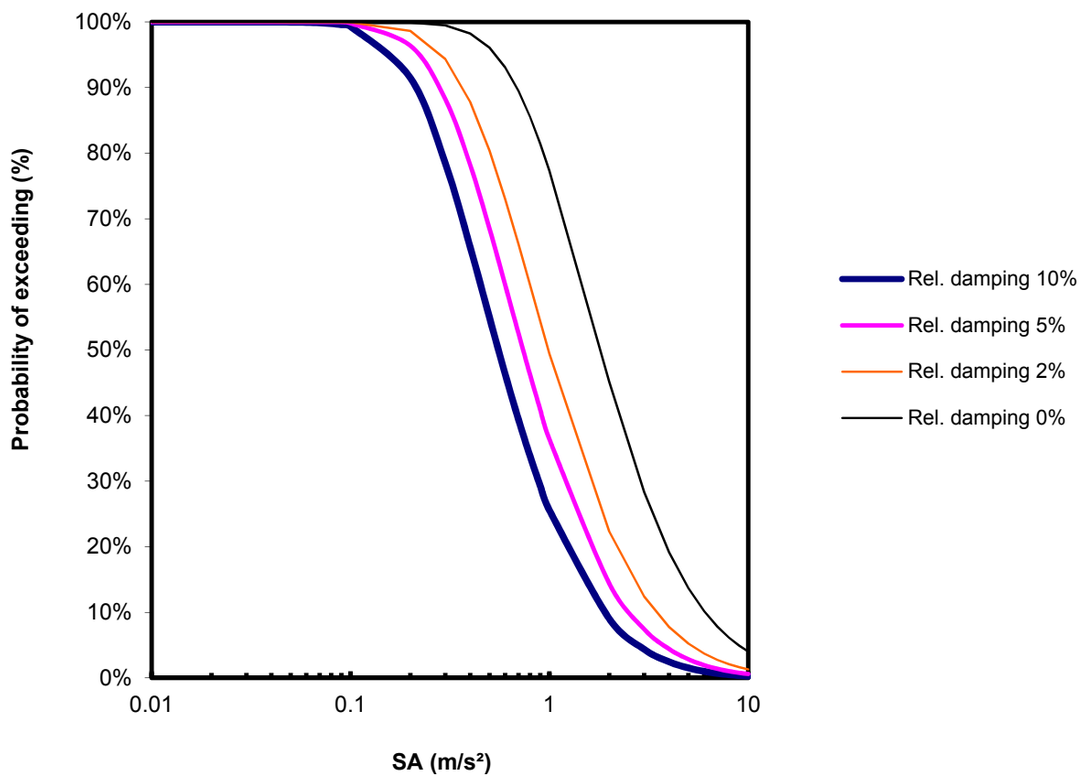

Fig. 7. Comparison for different damping ratios of the seismic hazard plot for the acceleration response spectrum. Period 0.20. s, in rock with a time of exposure of 50 years and for Granada.

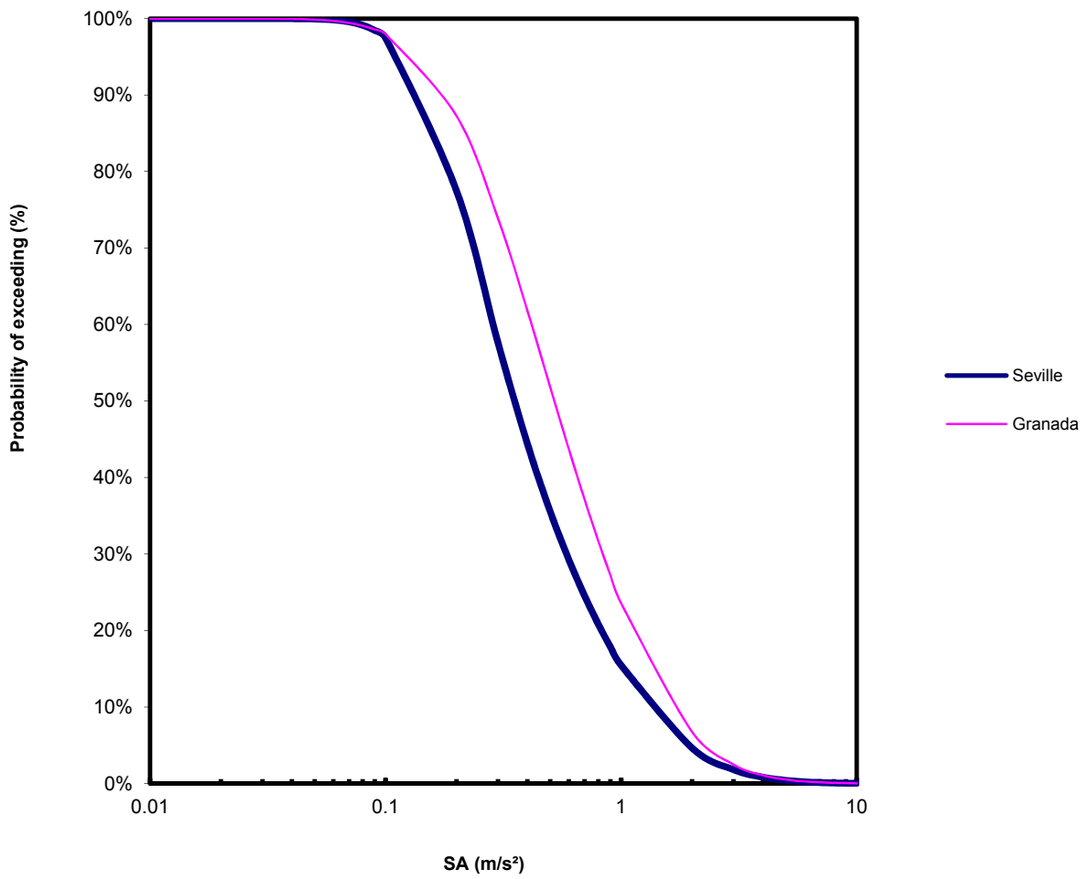

Fig. 8. Comparison of the seismic hazard plots of the acceleration response spectra between Seville and Granada. Period 0.50 s, hard soil, 5% relative dumping and a time of exposure of 50 years.

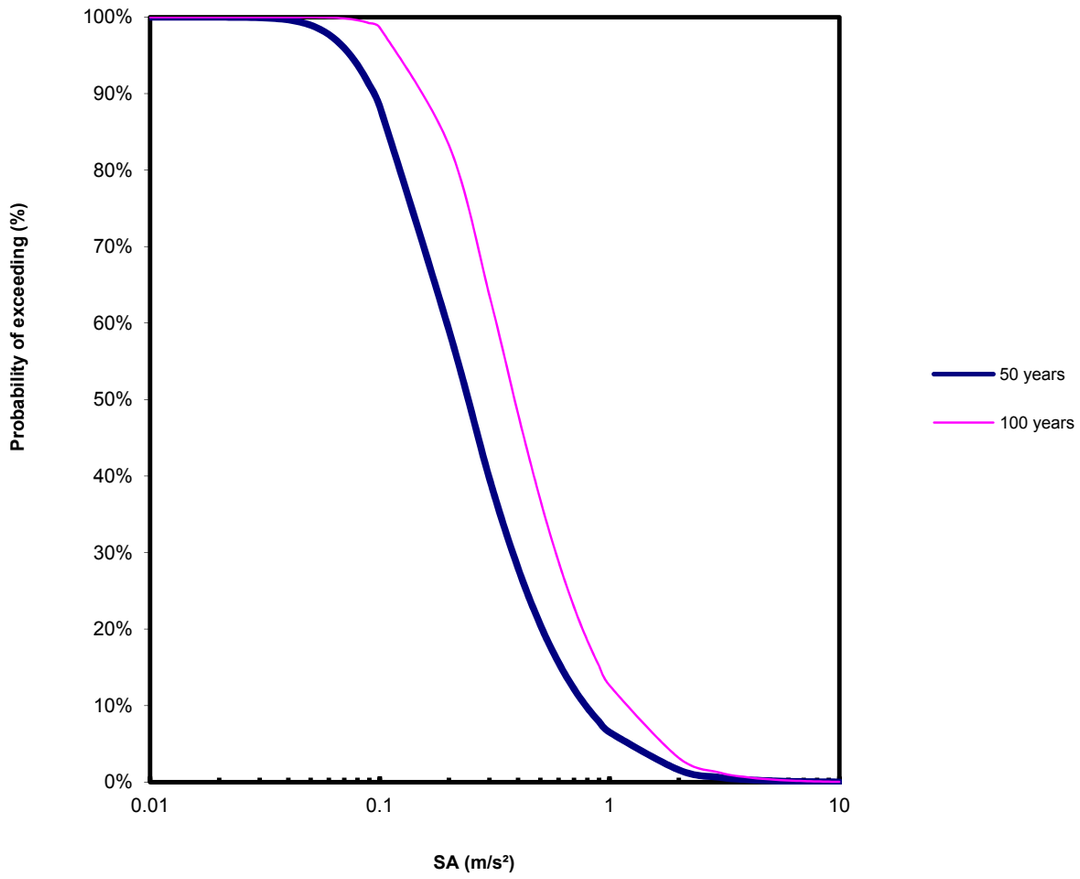

Fig. 9. Comparison for different exposure times of the seismic hazard plot of the acceleration response spectrum. Granada site for a 0.50 s period, in rock and a 5% relative dumping.

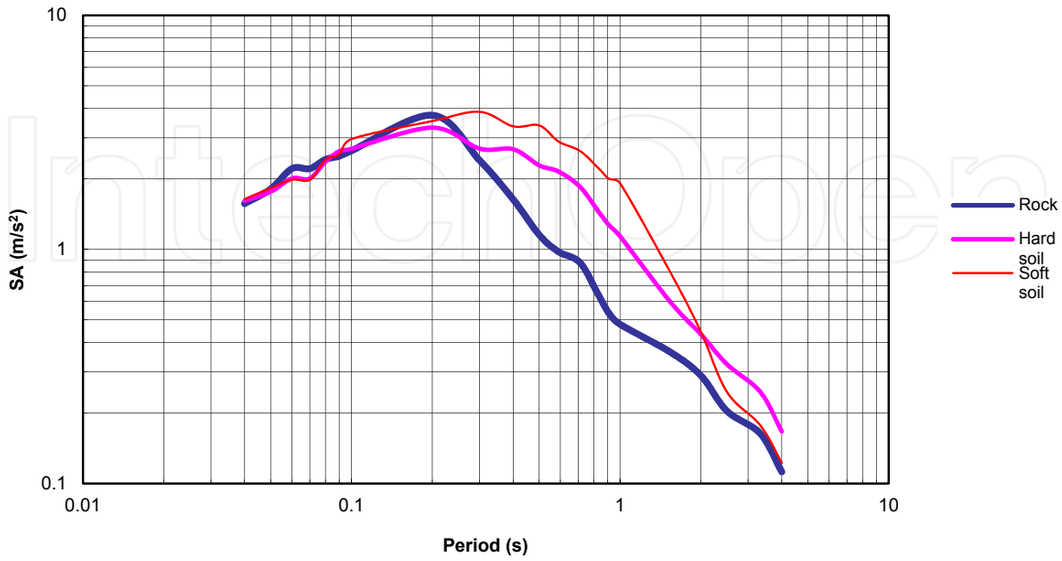

Fig. 10. Comparison of the uniform seismic hazard acceleration response spectra for different soil types. Granada site, probability of being exceeded 5%, relative damping 5% and time of exposure 50 years.

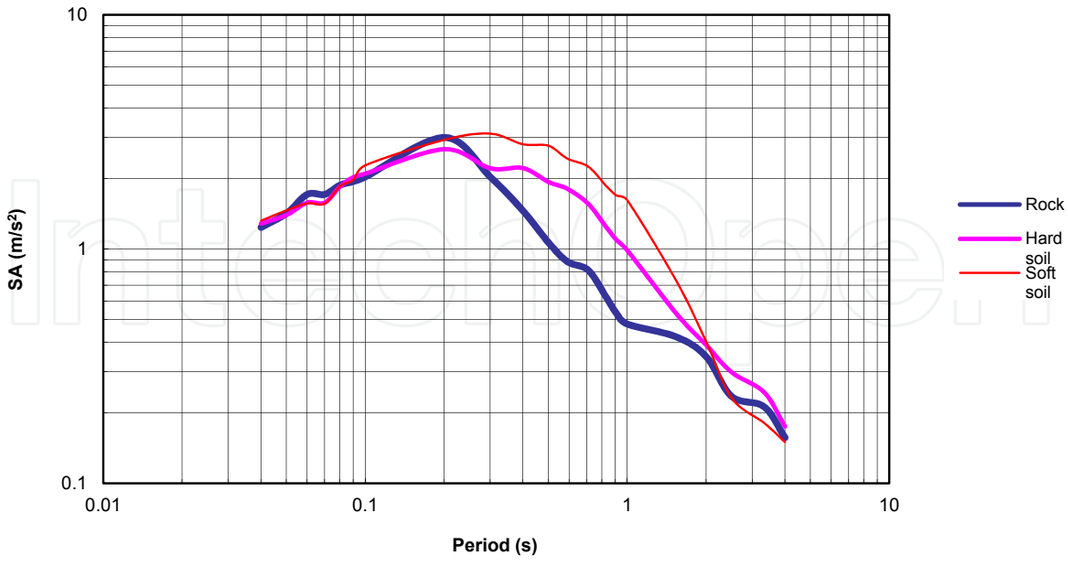

Fig. 11. Comparison of the uniform seismic hazard acceleration response spectra for different soil types. Seville site, probability of being exceeded 5%, relative damping 5% and time of exposure 50 years.

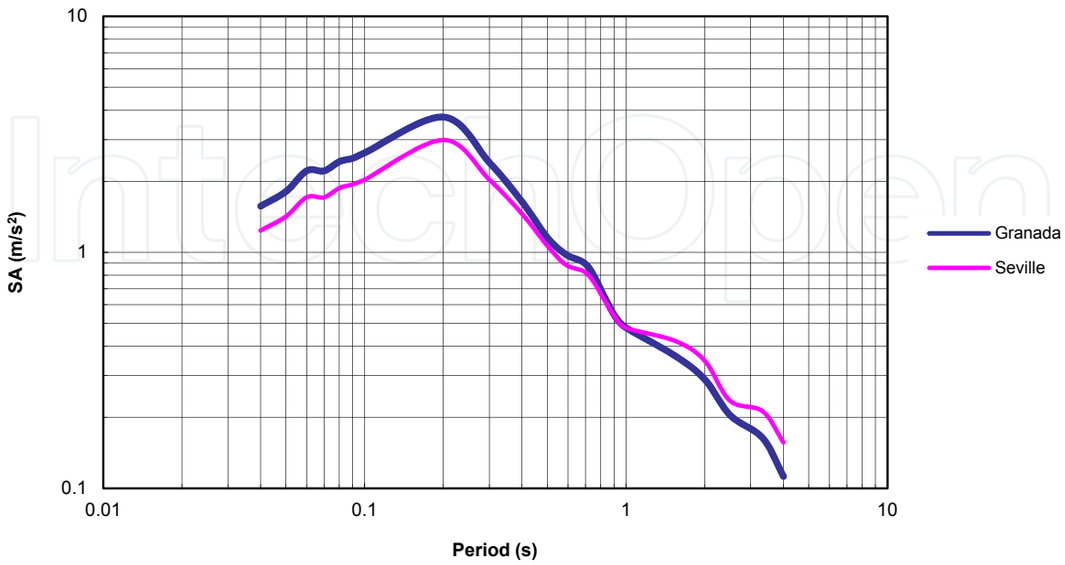

Fig. 12. Comparison between Seville and Granada of the uniform seismic hazard acceleration response spectrum in rock. Probability of being exceeded 5%, relative dumping 5% and time of exposure 50 years.

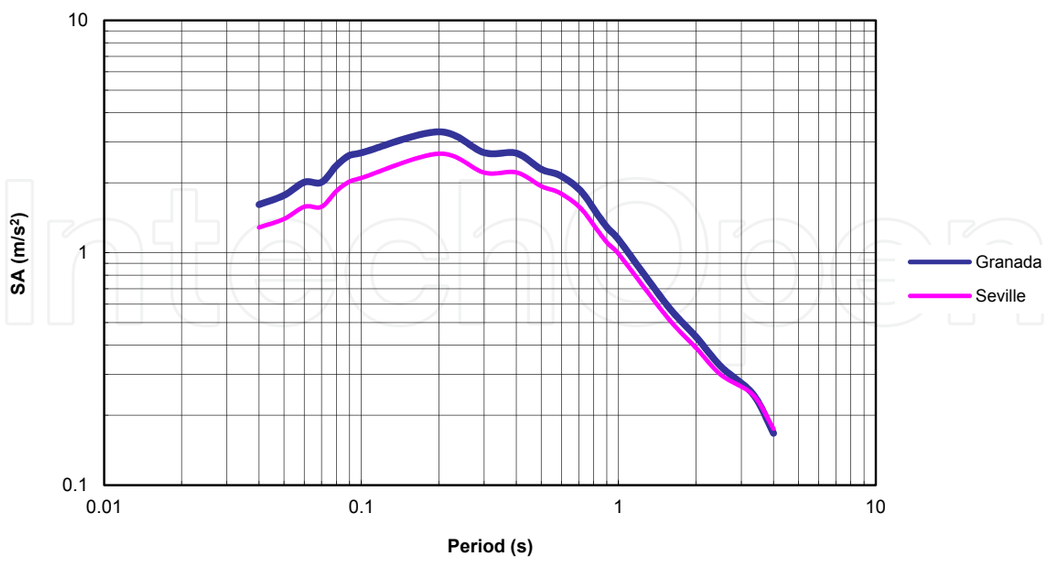

Fig. 13. Comparison between Seville and Granada of the uniform seismic hazard acceleration response spectrum in hard soil. Probability of being exceeded 5%, relative dumping 5% and time of exposure 50 years.

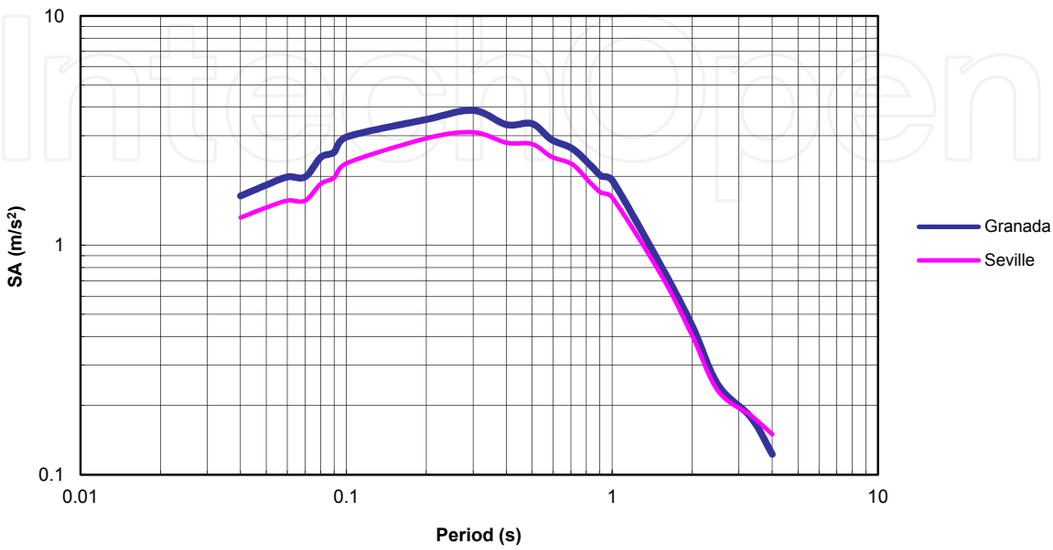

Fig. 14. Comparison between Seville and Granada of the uniform seismic hazard acceleration response spectrum in soft soil. Probability of being exceeded 5%, relative dumping 5% and time of exposure 50 years.

3.4.1 Estimation of calculation accelerograms for San Pedro Cliff at the Alhambra (Granada)

As an example of the methodology presented in this paper calculation accelerograms for San Pedro Cliff at the Alhambra of Granada are obtained. First, the acceleration response spectrum for San Pedro Cliff is calculated in rock (V_s≥750 m/s), for a probability of exceeding of the 5% and a time of exposure of 50 years, which is equivalent to a return period of 975 years. The accelerograms have been obtained from the European earthquake database that can be consulted from the internet: http://www.isesd.cv.ic.ac.uk/.

the Alhambra in Granada is one of the most important national monuments in Spain. This monument, a World Heritage site, is located on the top of a red hill that dominates a plain, the Granada basin, where most of the city is placed. One of the most important rivers of the region, River Darro, flows into the basin and is situated on the western part of the city. The Alhambra's walls are close to the escarpments generated by the incision of this river. Slope instability of the escarpments on this side of the Alhambra hill has been a critical problem since the construction of this palace. In this area, San Pedro Cliff (figure 15), a dihedral 65.5 m high, is the steepest escarpment of the Alhambra hill. This eroding cliff reaches to 23.8 m from the Alhambra palace wall. Retreat of this cliff has occurred

through superficial slab falls mainly induced by the floods of the Darro River, the loosening produced by the extensional tectonic regime, erosion, seepage coming from the Alhambra palace and earthquakes.

Granada basin presents several sets of faults, most notably those E-W and NW-SE orientations. Conspicuous NW-SE faults are present in the eastern part of the basin, some of which limit the Granada basin. These faults are normal, mostly with a NW-SE orientation, and dipping towards the SW. These NW-SE faults cross-cut and displace previous E-W faults, defining the main subsiding areas of the central and eastern part of the basin.

Fig. 15. South view of San Pedro Cliff, showing to the right the fault line scarp. Above stand the Alhambra walls and, at the foot, River Darro and Albaicín houses

A site investigation was conducted by (Justo et al., 2008). The following layers appear from top to bottom in the geological profile:

1. Dense conglomerate. V_s=800 m/s (transverse wave velocity).
2. Very dense conglomerate. V_s=960 m/s.
3. Moderately dense conglomerate. V_s=800 m/s.
4. Very dense, gravelly and sandy conglomerate. V_s=1150 m/s.

4a. One meter thick clay layers, interspersed in layer 4. V_s=800 m/s.

Talus appears at the foot of the slope, composed of quartzose and phyllitic blocks, gravel and sand, with predominance of the sand fraction.

Figures 16 to 25 represent the uniform seismic hazard acceleration response spectra for San Pedro Cliff at the Alhambra of Granada and the response spectra of the real earthquakes with better adjustment. The scaled spectrum that minimizes the standard deviation has also been plotted. The records data that minimize the standard deviation are shown in Tables 3 and 4.

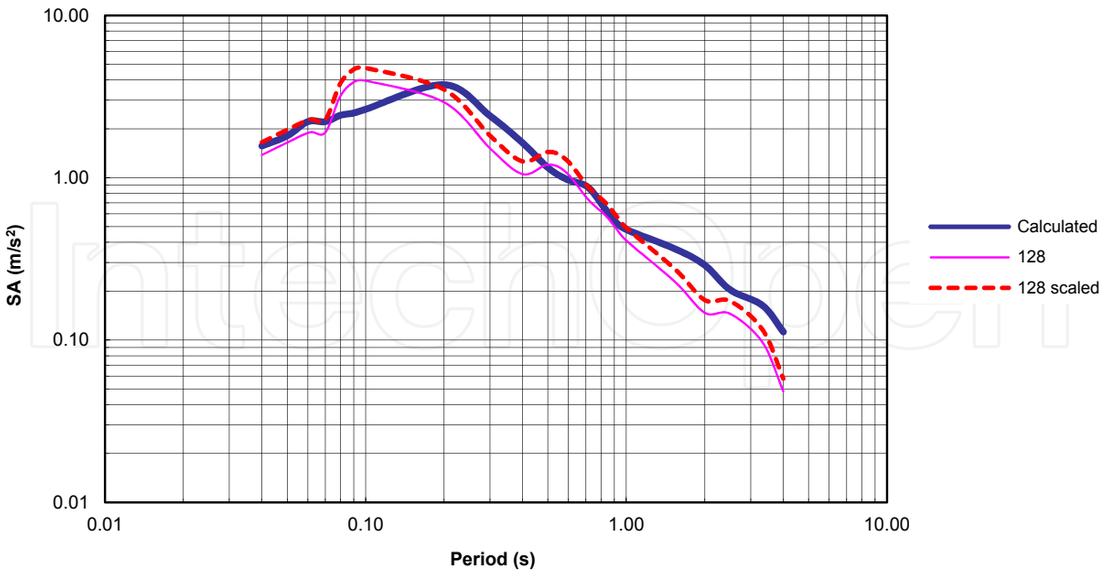

Fig. 16. Seismic hazard acceleration response spectra for San Pedro cliff at the Alhambra in Granada. Probability of being exceeded 5%, relative dumping 5%, rock, time of exposure 50 years. Comparison between the calculated uniform acceleration response spectrum, the spectrum corresponding to record 128 from the catalogue and the spectrum scaled to minimize the standard deviation.

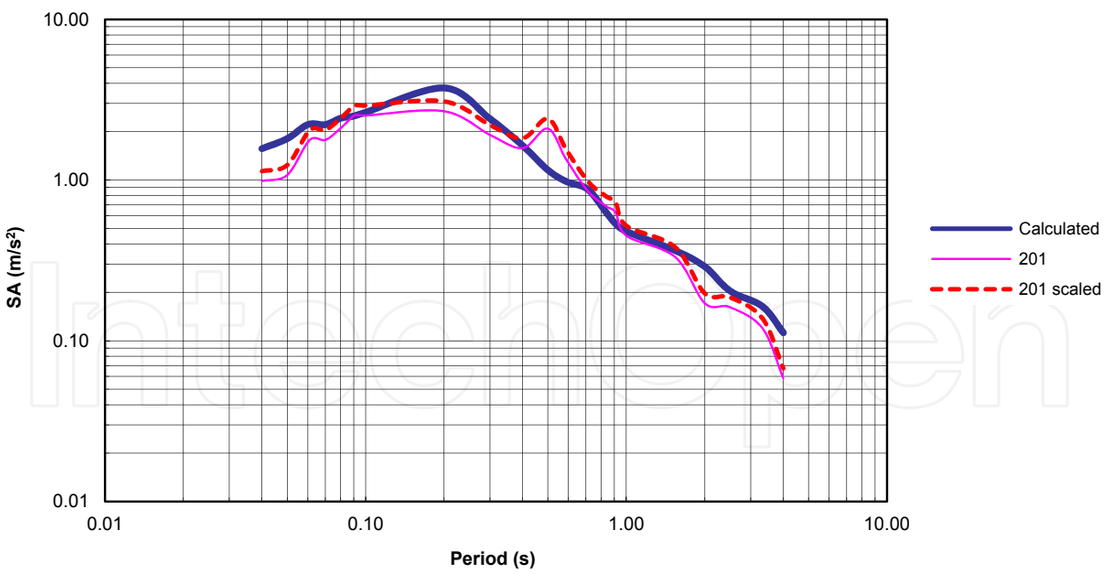

Fig. 17. Seismic hazard acceleration response spectra for San Pedro cliff at the Alhambra in Granada. Probability of being exceeded 5%, relative dumping 5%, rock, time of exposure 50 years. Comparison between the calculated uniform response spectrum, the spectrum corresponding to record 201 from the catalogue and the spectrum scaled to minimize the standard deviation.

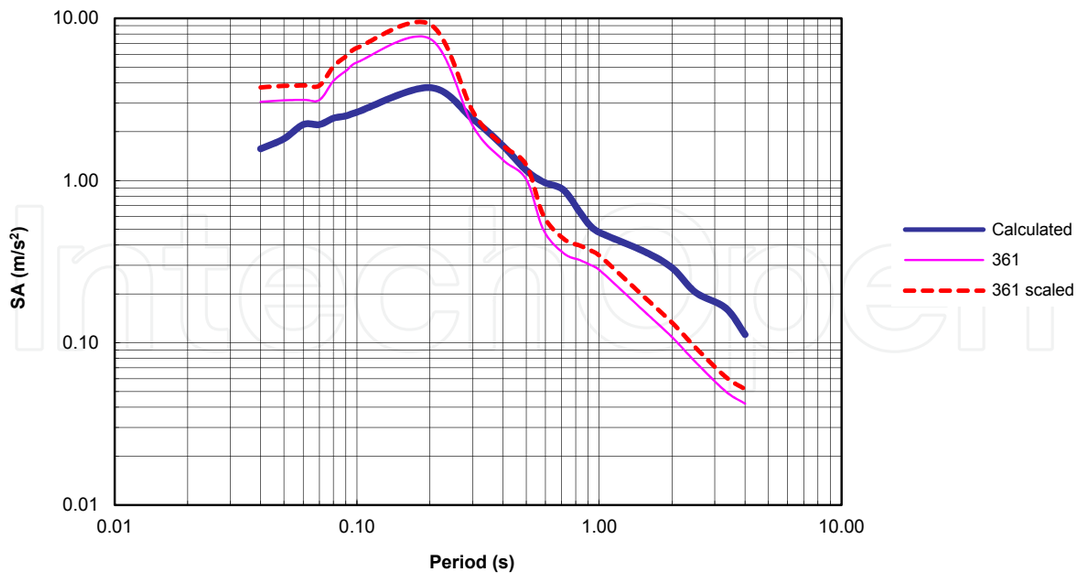

Fig. 18. Seismic acceleration response spectra for San Pedro cliff at the Alhambra (Granada). Probability of being exceeded 5%, relative dumping 5%, rock, time of exposure 50 years. Comparison between the calculated uniform response spectrum, the spectrum corresponding to record 361 and the spectrum scaled to minimize the standard deviation.

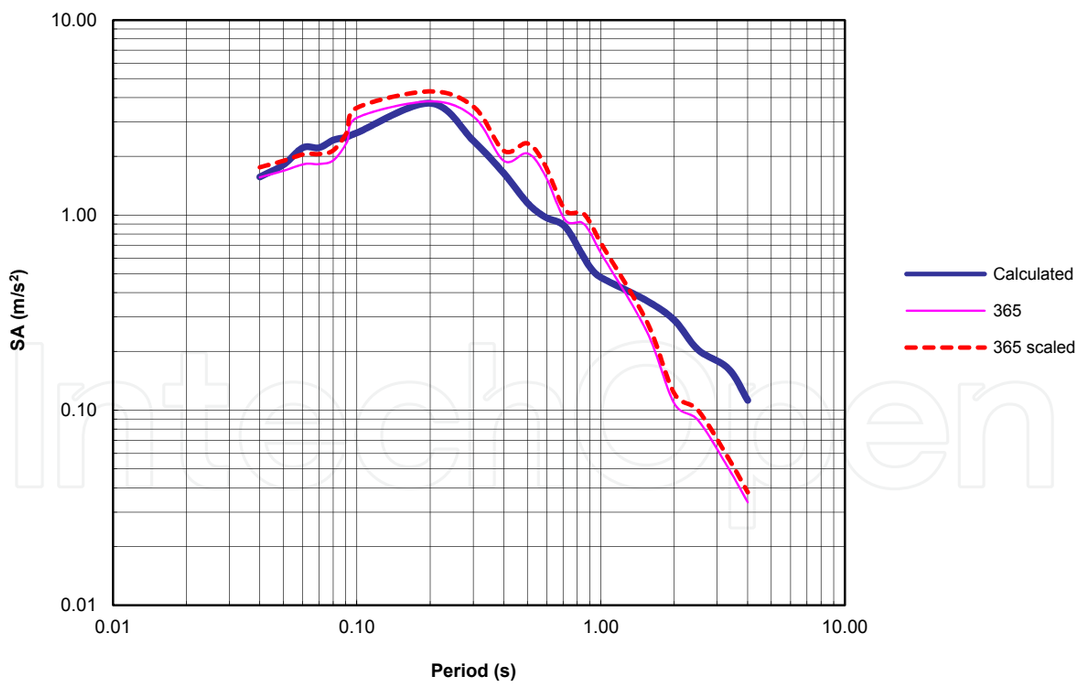

Fig. 19. Seismic acceleration response spectra for San Pedro cliff at the Alhambra (Granada). Probability of being exceeded 5%, relative dumping 5%, rock, time of exposure 50 years. Comparison between the calculated uniform response spectrum, the spectrum corresponding to record 365 and the spectrum scaled to minimize the standard deviation.

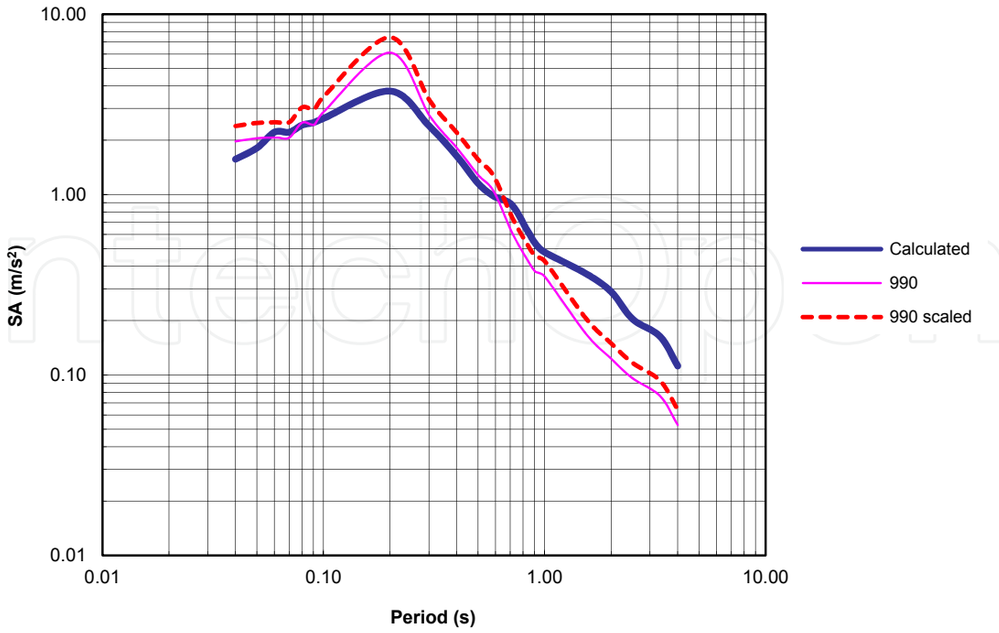

Fig. 20. Seismic acceleration response spectra for San Pedro cliff at the Alhambra (Granada). Probability of being exceeded 5%, relative dumping 5%, rock, time of exposure 50 years. Comparison between the calculated uniform response spectrum, the spectrum corresponding to record 990 and the spectrum scaled to minimize the standard deviation.

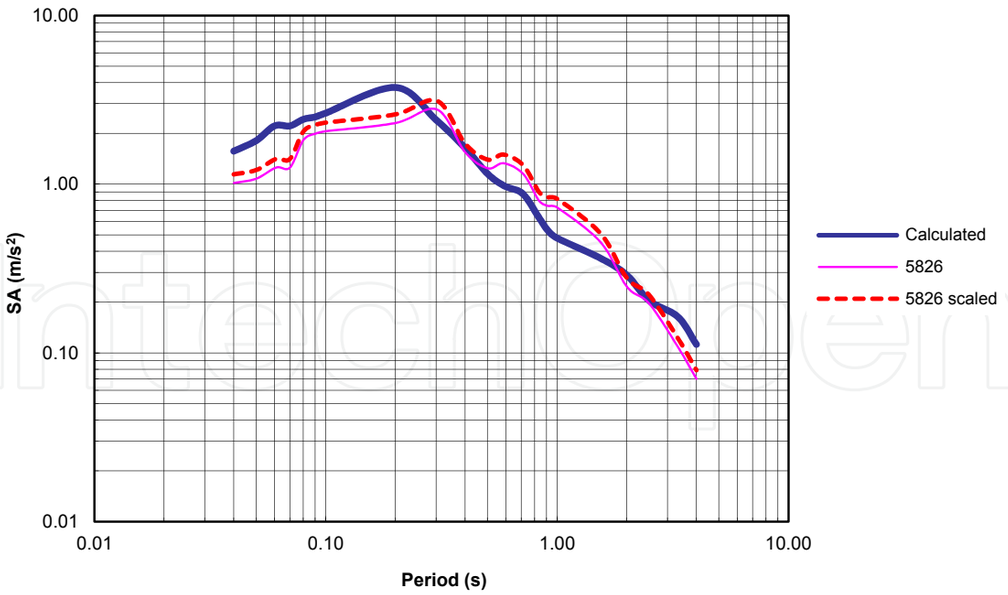

Fig. 21. Seismic acceleration response spectra for San Pedro cliff at the Alhambra (Granada). Probability of being exceeded 5%, relative dumping 5%, rock, time of exposure 50 years. Comparison between the calculated uniform response spectrum, the spectrum corresponding to record 5826 and this spectrum scaled to minimize the standard deviation.

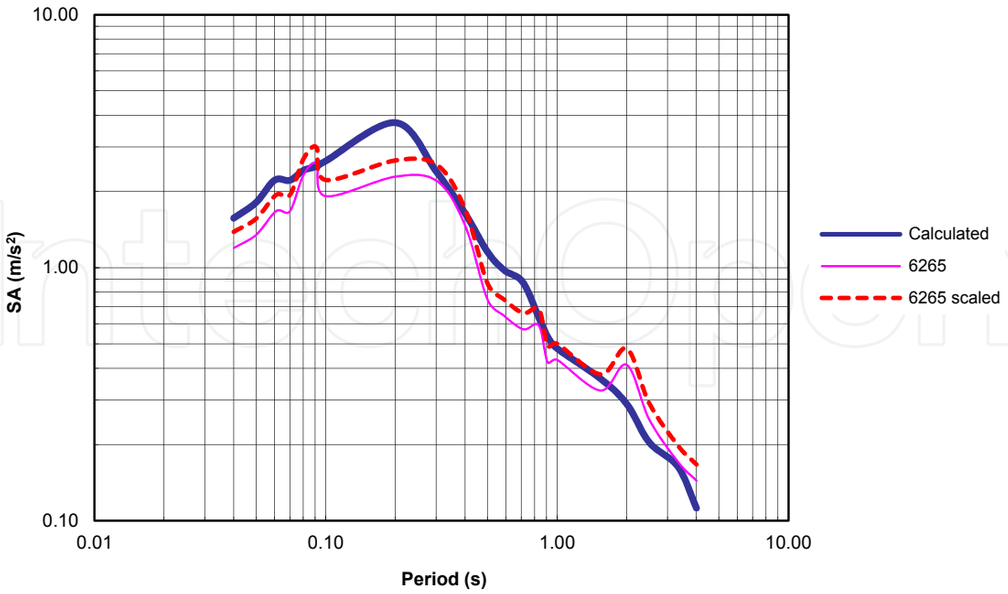

Fig. 22. Seismic acceleration response spectra for San Pedro cliff at the Alhambra (Granada). Probability of being exceeded 5%, relative dumping 5%, rock, time of exposure 50 years. Comparison between the uniform response spectrum, the spectrum corresponding to record 6265 and the spectrum scaled to minimize the standard deviation.

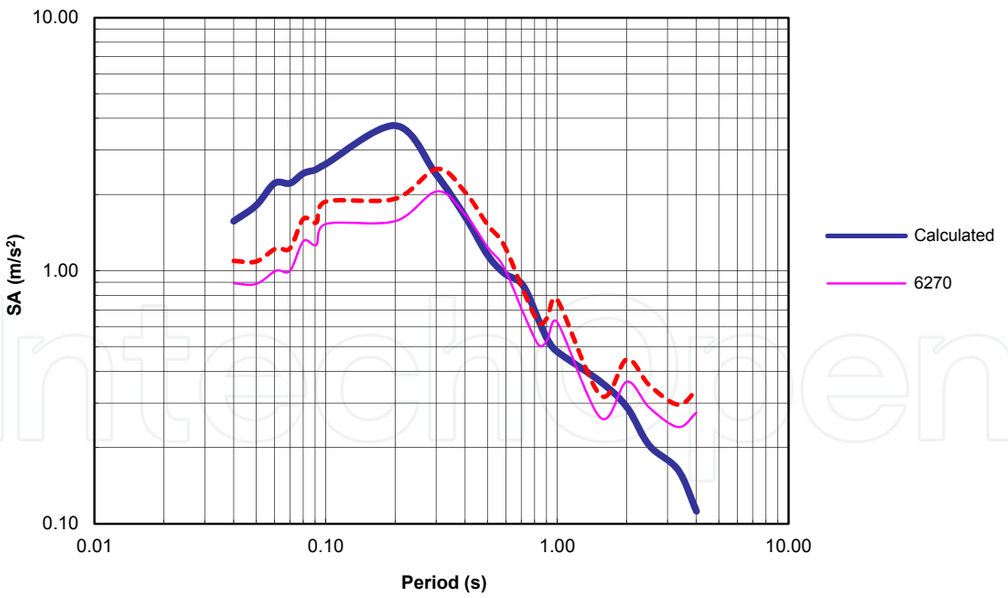

Fig. 23. Seismic acceleration response spectra for San Pedro cliff at the Alhambra (Granada). Probability of being exceeded 5%, relative dumping 5%, rock, time of exposure 50 years. Comparison between the calculated uniform response spectrum, the spectrum corresponding to record 6270 and the spectrum scaled to minimize the standard deviation.

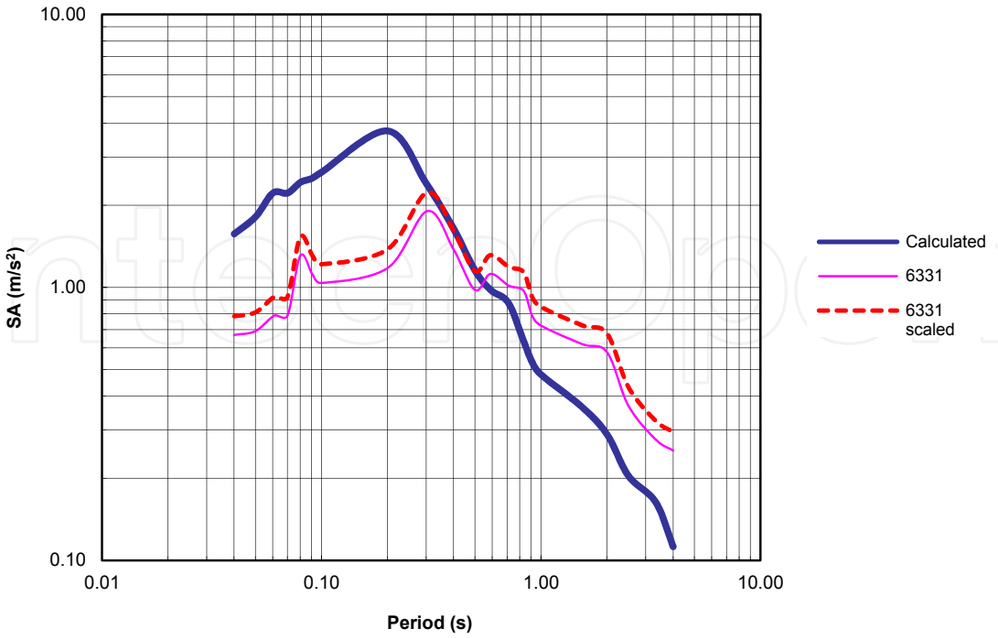

Fig. 24. Seismic acceleration response spectra for San Pedro cliff at the Alhambra (Granada). Probability of being exceeded 5%, relative dumping 5%, rock, time of exposure 50 years. Comparison between the calculated uniform response spectrum, the spectrum corresponding to record 6331 and the spectrum scaled to minimize the standard deviation.

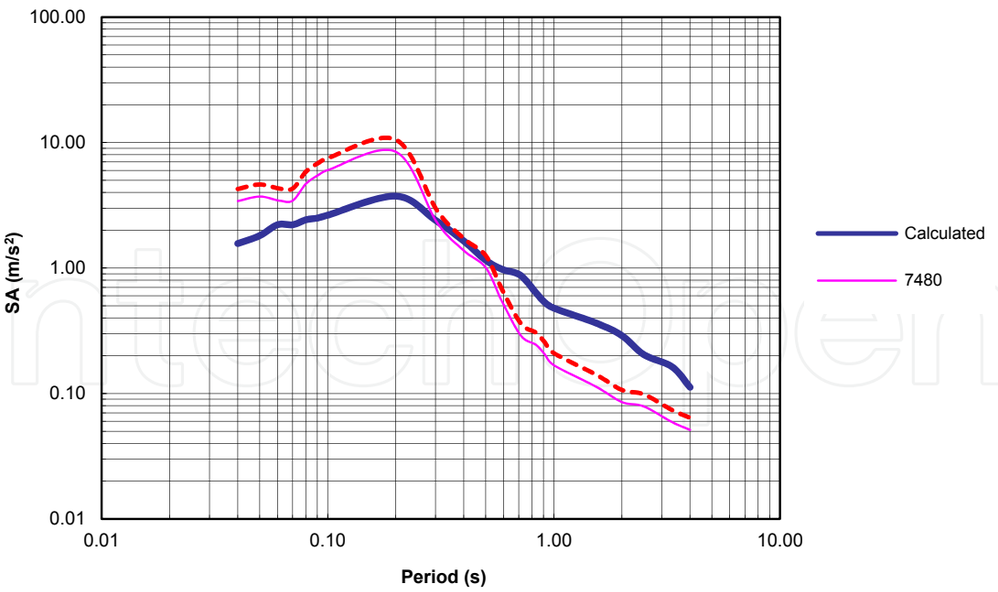

Fig. 25. Seismic acceleration response spectra for San Pedro cliff at the Alhambra (Granada). Probability of being exceeded 5%, relative dumping 5%, rock, time of exposure 50 years. Comparison between the calculated uniform response spectrum, the spectrum corresponding to record 7480 and the spectrum scaled to minimize the standard deviation.

Earthaquake record	**128**
Seismic data	
Earthquake:	Friuli (Northern Italy)
Date:	9/15/1976
Magnitude:	6.0 M_w
Record data	
Station:	Robic (Slovenia)
Type of soil:	Rock
Fault distance:	19
f	1.2
s	0.016
$SA_{max}(m/s^2)$	3.96

Earthaquake record	**201**
Seismic data	
Earthquake:	Montenegro (Adriatic Sea)
Date:	4/15/1979
Magnitude:	6.9 M_w
Record data	
Station:	Dubrovnik-Pomorska School (Croatia)
Type of soil:	Rock
Fault distance:	61
f	1.15
s	0.087
$SA_{max}(m/s^2)$	2.68

Earthaquake record	**361**
Seismic data	
Earthquake:	Umbria (Center of Italy)
Date:	4/19/1984
Magnitude:	5.6 M_w
Record data	
Station:	Nocera Umbra (Italy)
Type of soil:	Rock

Fault distance:	19
f	1.23
s	0.028
$SA_{max}(m/s^2)$	7.49

Earthaquake record	**365**
Seismic data	
Earthquake:	Lazio Abruzzo (Southern Italy)
Date:	5/7/1984
Magnitude:	5.9 M_w
Record data	
Station:	Atina (Italy)
Type of soil:	Rock
Fault distance:	11
f	1.12
s	0.13
$SA_{max}(m/s^2)$	3.83

Earthaquake record	**990**
Seismic data	
Earthquake:	Lazio Abruzzo, aftershock (Southern Italy)
Date:	5/11/1984
Magnitude:	5.5 M_w
Record data	
Station:	Atina-Pretura Terrazza (Italy)
Type of soil:	Rock
Fault distance:	13
f	1.22
s	0.011
$SA_{max}(m/s^2)$	6.11

Table 3. Information about the records whose typical deviation is minor in relation to the uniform seismic hazard acceleration response spectra for San Pedro Cliff at the Alhambra in Granada for a 5% probability of being exceeded, an exposure time of 50 years over rock and a relative damping of the 5%

Earthaquake record	5826
Seismic data	
Earthquake:	Strofades (Jonic Sea)
Date:	11/18/1997
Magnitude:	6.6 M_w
Record data	
Station:	Kyparrisia-Agriculture Bank (Greece)
Type of soil:	Rock
Fault distance:	65
f	1.13
s	0.129
$SA_{max}(m/s^2)$	2.76

Earthaquake record	6265
Seismic data	
Earthquake:	Southern Iceland
Date:	6/17/2000
Magnitude:	6.5 M_w
Record data	
Station:	Burfell Hydroelectric Station (Iceland)
Type of soil:	Rock
Fault distance:	25
f	1.16
s	0.076
$SA_{max}(m/s^2)$	2.58

Earthaquake record	6270
Seismic data	
Earthquake:	Suthern Iceland
Date:	6/17/2000
Magnitude:	6.5 M_w
Record data	
Station:	Ljosafoss Hydroelectric Station (Iceland)
Type of soil:	Rock

Fault distance:	32
f	1.23
s	0.026
$SA_{max}(m/s^2)$	2.06

Earthaquake record	6331
Seismic data	
Earthquake:	Southern Iceland, aftershock
Date:	6/21/2000
Magnitude:	6.4 M_w
Record data	
Station:	Flagbjarholt (Iceland)
Type of soil:	Rock
Fault distance:	22
f	1.17
s	0.057
$SA_{max}(m/s^2)$	1.90

Earthaquake record	7480
Seismic data	
Earthquake:	St. Die (France)
Date:	2/22/2003
Magnitude:	4.7 M_w
Record data	
Station:	Bremgarten (Germany)
Type of soil:	Rock
Fault distance:	-
f	1.25
s	0.058
$SA_{max}(m/s^2)$	8.45

Table 4. Information about the records whose typical deviation is minor in relation to the uniform seismic hazard acceleration response spectra for San Pedro Cliff at the Alhambra in Granada for a 5% probability of being exceeded, an exposure time of 50 years over rock and a relative damping of the 5%

4. Conclusions

The proposed method to obtain design accelerograms provides real accelerograms, registered in the same type of soil of the location and compatible with the uniform seismic hazard response spectra calculated at the site.

It can be observed from the comparison of the uniform seismic hazard acceleration response spectra for Seville and Granada, as a function of the type of soil (Figures 10 and 11), that for periods minor to 0.20 s there is almost no difference between the different type of soils. The difference has a maximum for the intermediate periods (0.40 to 1.00 s) and disappears for the periods over 2.00 s. The maximum value for the acceleration response spectrum is obtained for periods between 0.20-0.30 s.

From the comparison between Seville and Granada for different soil types (fig. 12 to 14) the following can be concluded: for longer periods the acceleration response spectra converge. The maximum value for rock and hard soil is obtained for a period of 0.20 s. For soft soil and very soft soil, the maximum of the acceleration response spectra is for 0.30 s.

The proposed method to estimate calculation accelerograms has been used for San Pedro Cliff at the Alhambra in Granada for a return period of 975 years. The results are presented in Figures 16 to 25. The type of soil at the site is rock. The site investigation has shown a transverse wave velocity for the cliff of over 800 m/s. Tables 3 to 4 provide information about the earthquake records that better fit the uniform seismic hazard spectrum. It can be observed the good adjustment obtained as the standard deviation is very low, with a minimum of 0.011 for the register 990.

5. Acknowledgements

The financial support given by the Spanish Ministry of Science and Technology, projects BIA-2004-01302 and BIA2010-20377 is acknowledged. The authors also want to acknowledge Mr. Antonio Jesús Martín for providing the Spanish database of earthquakes.

6. References

Benito, B. & Jiménez, M. E. (1999). Peligrosidad sísmica, *Física de la Tierra,* 11, pp. 1-28.

Cornell, C. A. (1968). Engineering seismic risk analysis, *Bulletin of the Seismological Society of America*, Vol.58, pp. 1583-1606.

Ebel, J. E. & Kafka, A. L. (1999). A Monte Carlo approach to seismic hazard analysis, *Bulletin of the Seismological Society of America*, Vol.89, pp. 854-866.

Gumbel, E. J. (1958). *Statistics of extremes*, Columbia university press, New York, 1958.

Housner, G. W. (1975). Spectrum intensities of strong motion earthquakes, *Proceedings of the symposium on earthquake and blast effects on structures*, EERI.

Justo, J. L.; Azañón, J.M.; Azor, A.; Saura, J.; Durand, P.; Villalobos, M.; Morales-Esteban, A. & Justo E. (2008), Neotectonics and slope stabilization at the Alhambra, Granada, Spain, *Engineering Geology*, Vol.100, pp. 101-119.

Lin, J. & Mahin, S.A. (1985). Effect of inelastic behavior on the analysis and design of earthquake resistant structures, *Earthquake engineering*.

Martín, A. J. (1984). Riesgo sísmico en la Península Ibérica, *Thesis*, Universidad Politécnica de Madrid.

Meirovitch, L. (1985). *Introduction to dynamics and control*, John Wiley & Sons, Inc., New York.

Morales-Esteban, A. (2010). Peligrosidad sísmica. Leyes de atenuación y análisis de las series temporales de los terremotos. Aplicación al Tajo de San Pedro de la Alhambra de Granada, *Thesis*, Universidad de Sevilla, Sevilla.

UNDRO, 1979. Natural disasters and vulnerability analysis*, Report expert group meeting*, Geneva.

Veneziano, D.; Cornell, C. A. & O´Hara, T. (1984). *Historical methods of seismic hazard analysis*, Electric power research institute, Palo Alto, California, Research Report NP-3438.

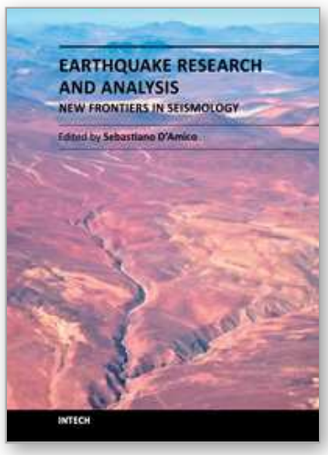

Earthquake Research and Analysis - New Frontiers in Seismology
Edited by Dr Sebastiano D'Amico

ISBN 978-953-307-840-3
Hard cover, 380 pages
Publisher InTech
Published online 27, January, 2012
Published in print edition January, 2012

The study of earthquakes combines science, technology and expertise in infrastructure and engineering in an effort to minimize human and material losses when their occurrence is inevitable. This book is devoted to various aspects of earthquake research and analysis, from theoretical advances to practical applications. Different sections are dedicated to ground motion studies and seismic site characterization, with regard to mitigation of the risk from earthquake and ensuring the safety of the buildings under earthquake loading. The ultimate goal of the book is to encourage discussions and future research to improve hazard assessments, dissemination of earthquake engineering data and, ultimately, the seismic provisions of building codes.

InTech Europe
University Campus STeP Ri
Slavka Krautzeka 83/A
51000 Rijeka, Croatia
Phone: +385 (51) 770 447
Fax: +385 (51) 686 166
www.intechopen.com

InTech China
Unit 405, Office Block, Hotel Equatorial Shanghai
No.65, Yan An Road (West), Shanghai, 200040, China
中国上海市延安西路65号上海国际贵都大饭店办公楼405单元
Phone: +86-21-62489820
Fax: +86-21-62489821

IntechOpen